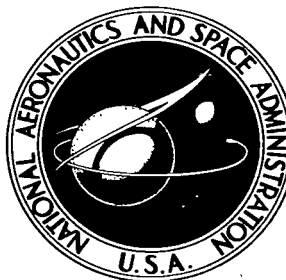


**NASA TECHNICAL NOTE**



**NASA TN D-2726**

**NASA TN D-2726**



# **AN ON-OFF CONTROL SYSTEM FOR A ROTATING MANNED SPACECRAFT**

*by Peter R. Kurzhals and John G. Shearin*

*Langley Research Center*

*Langley Station, Hampton, Va.*



AN ON-OFF CONTROL SYSTEM FOR A  
ROTATING MANNED SPACECRAFT

By Peter R. Kurzhals and John G. Shearin

Langley Research Center  
Langley Station, Hampton, Va.

NATIONAL AERONAUTICS AND SPACE ADMINISTRATION

---

For sale by the Office of Technical Services, Department of Commerce,  
Washington, D.C. 20230 -- Price \$2.00

# AN ON-OFF CONTROL SYSTEM FOR A

## ROTATING MANNED SPACECRAFT

By Peter R. Kurzhals and John G. Shearin  
Langley Research Center

### SUMMARY

A pulse-jet damping and attitude control system suitable for a rotating manned spacecraft has been investigated. The pulse-jet stability system has been simulated analytically in the nonlinear equations of motion for the spacecraft, and the efficiency of the stability system in controlling the spacecraft wobble and attitude is determined by digital integration.

To give physical significance to the results, typical motion time histories are presented for a large-diameter symmetric space station. In addition, the time to damp and the fuel required by the stability system are given for a range of system variables and spacecraft inertias.

The pulse-jet system is capable of rapidly minimizing any spacecraft wobble resulting from applied disturbances, such as crew motions and docking torques, to a steady spin about the spacecraft principal maximum or minimum axis of inertia. The system is also capable of readily reorienting the spinning spacecraft and can thus serve for combined attitude control and wobble damping.

### INTRODUCTION

Present concepts for rotating manned spacecraft, such as that shown in figure 1, in general require that the spacecraft spin uniformly and simultaneously maintain a specified attitude in space. Any undamped wobbling motions and attitude errors that may arise from personnel movements, docking impacts, and other disturbances (refs. 1 to 3) should be minimized. Attitude control and wobble damping will thus be required for such spacecraft.

A number of systems for wobble damping have been developed. (See refs. 4 to 6.) These systems, in general, provide only damping moments and cannot change the orientation of the rotating spacecraft. For missions which require attitude control, an additional system must then be provided. If this system produces both attitude and damping torques, a single stability system will suffice for the spacecraft, and the weight of the control system may be less than that for previously considered systems.

The present study investigates a pulse-jet system which can be used for either damping or attitude control, as well as for combined operation. The pulse-jet system can thus function independently or in conjunction with a wobble-damping system. Command signals for the automatically controlled system are taken from rate gyros and a sunseeker or an inertial platform within the spacecraft.

## SYMBOLS

A	absolute value of deadband imposed on station rate errors by pulse-jet stability system, radians/sec
B	absolute value of deadband imposed on station attitude errors by pulse-jet stability system, deg
I	in-plane moment of inertia, $I_X$ or $I_Y$ , slug-ft <sup>2</sup>
$I_S$	specific impulse, lb/lb/sec
$I_Z$	spin moment of inertia, slug-ft <sup>2</sup>
$I_{XZ}$	product of inertia in XZ body plane, slug-ft <sup>2</sup>
l	moment arm, ft
$M_d$	damping moment, ft-lb
M	moment, $I_Z \Omega_Z^2$ , ft-lb
t	time, sec
U	inclination angle between the Z body axis and a fixed reference line, deg (fig. 3)
V	angle between the X body axis and a plane perpendicular to the fixed reference line, deg (fig. 3)
W	angle between the Y body axis and a plane perpendicular to the fixed reference line, deg (fig. 3)
$W_F$	fuel weight required by pulse-jet system, lb
$W_{F,0}$	reference fuel weight, $I_Z \Omega_Z / I_S l$ , lb
X,Y,Z	station body axes used for analysis, with the Z-axis selected as spin axis
$\alpha$	angular position, deg

$\gamma$	inertia ratio, $\frac{I}{I_Z}$
$\epsilon_f$	fuel weight ratio, $\frac{W_f}{W_{f,o}}$
$\lambda$	nondimensional moment, $\frac{M}{M_o}$
$\tau$	time, $t\Omega_Z$ , sec
$\phi, \theta, \psi$	Euler angles
$\Omega$	angular velocity, radians/sec
$\omega$	nondimensional angular velocity, $\Omega/\Omega_Z$

Subscripts:

a	applied
av	average
b	body
d	damping
db	deadband
fs	fixed space
o	reference

X,Y,Z components parallel to X-, Y-, Z-axis, respectively

A dot over a symbol denotes the derivative with respect to time.

A bar over a symbol denotes a vector.

A tilde ( $\sim$ ) over a symbol denotes a matrix.

## SYSTEM DESCRIPTION

The on-off stability control system (fig. 2) consists of four pulse jets equally spaced on the periphery and aligned parallel with the spacecraft spin axis. The jets are actuated by data giving the deviation of the station from a desired rate and attitude. For the damping phase, the angular velocities about the in-plane body axes are measured by rate gyros. These angular rates are fed

through an analog system that determines the average value of the rates and gives rate error from an average value. A deadband is then superimposed on the rate error. Whenever the rate error exceeds this deadband, the appropriate pulse jet is actuated to produce an opposing moment. The jet fires until the rate error gain passes into the deadband region and then cuts off. This procedure is repeated until the rate error is damped to the deadband region.

If attitude control is desired, the orientation phase of the pulse-jet system is actuated in conjunction with the damping phase. For this phase, a deadband is imposed on attitude errors which are determined by a sunseeker or inertial platform. While the attitude errors are outside this deadband, precessional torques are produced by the jets. When the applied torques have brought the station within the deadband ranges of both the orientation and damping phases, the stability system is again shut off.

It is assumed that the spacecraft spins about its Z-axis, so that the jets produce torques about the in-plane X- and Y-axes. Whenever a positive and negative torque about either of these two axes is called for simultaneously, the control logic cancels these opposing torques to minimize fuel consumption.

The effectiveness of the pulse-jet system in controlling the motions of the spacecraft has been studied through the use of the nonlinear equations of motion presented in the appendix. These equations describe the motion of an arbitrary rotating spacecraft with varying moments and products of inertia. Docking torques, mass unbalances, and transient crew motions are simulated in the equations, and a fourth-order Runge-Kutta integration procedure is used to determine the station motion. The damping moments exerted by the pulse-jet system are given by

$$\left. \begin{array}{ll} \lambda_X = -\lambda_{X,d} & \Delta\omega_X \geq A \\ \lambda_X = 0 & -A < \Delta\omega_X < A \\ \lambda_X = \lambda_{X,d} & \Delta\omega_X \leq -A \\ \lambda_Y = -\lambda_{Y,d} & \Delta\omega_Y \geq A \\ \lambda_Y = 0 & -A < \Delta\omega_Y < A \\ \lambda_Y = \lambda_{Y,d} & \Delta\omega_Y \leq -A \end{array} \right\} \quad (1)$$

Here the angular rate errors  $\Delta\omega$  are

$$\left. \begin{array}{l} \Delta\omega_X = \omega_X - \omega_{X,av} \\ \Delta\omega_Y = \omega_Y - \omega_{Y,av} \end{array} \right\} \quad (2)$$

with the average velocities  $\omega_{av}$  taken as the projections of the total angular-velocity vector on the spacecraft principal axes of inertia. In an actual system this average velocity can be measured by a dc pickup gage. Since the manned spacecraft will in general have continually changing moments and products of inertia, an equilibrium condition will exist when

$$\Delta\omega_X = \Delta\omega_Y = 0 \quad (3)$$

and the model is spinning about a maximum or minimum principal axis of inertia. The control system, which cuts off the jets only when this equilibrium condition is reached, then produces the desired damping.

The precession moments produced by the pulse-jet system can be written as

$$\left. \begin{array}{ll} \lambda_X = \lambda_{X,d} & V \geq B \\ \lambda_X = 0 & -B < V < B \\ \lambda_X = \lambda_{X,d} & V \leq -B \\ \lambda_Y = \lambda_{Y,d} & W \geq B \\ \lambda_Y = 0 & -B < W < B \\ \lambda_Y = \lambda_{Y,d} & W \leq -B \end{array} \right\} \quad (4)$$

where  $V$  and  $W$  denote the attitude errors of the  $X$  and  $Y$  body axes with respect to the desired attitude, as shown in figure 3. Since the precession moments would produce residual wobbling motions about the new spacecraft attitude, the pulse jets must apply combined precession and damping torques to achieve the desired spacecraft attitude. Both damping and orientation control phases are thus used for the station attitude control.

In this analysis it has been assumed that the thrust buildup and decay for the pulse jets would take place instantaneously. This assumption should closely approximate the behavior of the actual control jet. However, the elasticity of the spacecraft was not considered here.

## RESULTS AND DISCUSSION

The effects of typical disturbances with and without a jet stability system have been investigated for a space station such as that shown in figure 1. This configuration has the following approximate characteristics:

Orbital weight, lb . . . . .	137,000
Inertia ratio, $\gamma$ . . . . .	0.7
Spin inertia, $I_Z$ , slug-ft <sup>2</sup> . . . . .	15,000,000
Spin rate, $\Omega_Z$ , rpm . . . . .	3
Crew members . . . . .	21

The results of the study are given in figures 4 to 16.

Since the controlled station behavior becomes somewhat involved, it is desirable to examine characteristic time histories. Also the effects of a variation in the stability-system parameters for nutation damping, attitude control, and combined precession and nutation control should be examined separately.

#### NUTATION DAMPING

The primary excitations considered for the station are impulsive torques and mass shifts. These disturbances have been applied to the station to determine the efficiency of the jet system in nutation damping.

The effects of a pulse moment, characteristic of a docking or an attitude control torque, on the station motion are shown in figure 4. Without damping, the station experiences both attitude errors and an oscillation in the body rates  $\omega_X$  and  $\omega_Y$ . These are apparent as a rolling motion of the station floor. With the jet system, the station wobble is eliminated and a steady spin about a new axis in space results. This damping is accomplished in about six spin cycles.

Similarly, a product of inertia corresponding to an instantaneous movement of the crew to one extreme of the station, produces the results in figure 5. The undamped station again exhibits oscillations in both body rates and angular position. Upon actuation of the jets these oscillations are damped, until the station spins about its maximum axis of inertia. This damping, which takes approximately three spin cycles, then yields a small residual coning motion of the station, which should have no ill effects on the crew.

As a final disturbance, the crew was moved from one end of one of the six cylindrical modules of the station to the other end at a constant velocity of 7.24 ft/sec. The response of the station to this varying product-of-inertia disturbance is illustrated in figure 6. The resulting station wobble is again damped to a coning of the symmetry axis about the maximum axis of inertia in about two spin cycles.



## DAMPING SYSTEM PARAMETERS

Having examined typical station motions with the jet nutation damper, it is of interest to see how the jet system parameters affect the damping response. The basic system parameters here are taken as damping torque  $M_d$ , fuel consumption  $W_f$ , and time to damp  $t_{db}$ .

In practice the deadbands for this system must first be selected so that the station is within acceptable attitude and rate errors after damping to the deadband. The jet moment level should then be chosen such that this moment, when applied over the minimum firing time or time lag of the jets, will not cause the station to exceed the selected deadbands. If this were not done, the station would oscillate indefinitely about the deadbands and the jets would fire continuously. The resulting excessive fuel consumption is prohibitive.

With these restrictions in mind, the effect of the three basic fuel parameters may be evaluated. Since both time to damp to the deadband  $t_{db}$  and fuel consumption  $W_f$  are related to the damping-moment level  $M_d$  the nondimensionalized time and fuel consumption parameters  $\tau_{db}$  and  $\epsilon_f$  have been plotted against nondimensional moment  $\lambda_d$  for the product-of-inertia disturbance of figure 4. The result is shown in figure 7. It can be seen that an increase in damping torque produces a nonlinear decay in the time to damp. For small moments,  $\tau_{db}$  decreases rapidly as  $\lambda_d$  increases. A further increase in  $\lambda_d$  then results in smaller changes in  $\tau_{db}$ , which eventually reaches an approximately constant value independent of  $\lambda_d$ . Since the fuel consumption remained constant for all moment levels, it appears that the minimum damping time can be achieved by the maximum damping torque satisfying the deadband requirements.

It should be recalled that the stability system in figure 7 only uses rate inputs, and thus makes no attempt to minimize station attitude errors resulting from the disturbance. In an actual system, it may be desirable to minimize any attitude changes and to damp the station until it spins about its maximum inertia axis. This control can be approximately accomplished by also imposing an attitude deadband slightly larger than the maximum expected angular deviation of the maximum inertia axis from the symmetry axis of the station. The result, for the disturbance of figure 4, is presented in figure 8. The time to deadband  $\tau_{db}$  decreases from 300 seconds to 122 seconds as the moment level is increased from 0.00016 to 0.001. A further increase in  $\lambda_d$  results in a small change of  $\tau_{db}$ . The consumed fuel  $\epsilon_f$  decreases slightly to reach a minimum at  $\lambda_d = 0.00036$  and then increases with a further increase in  $\lambda_d$ . In a combined rate- and attitude-controlled system, lower damping torques and higher times to damp than for the purely rate controlled system may thus be necessary to minimize fuel consumption.

In some instances it appears advantageous to use a single-axis control, in which moments are exerted about only one axis of the station. This case is illustrated in figure 9 for the product-of-inertia disturbance of figure 4.

The station response is much the same as in the dual-axis case in figure 8 with the exception that, for the same control torque, the time to damp to the dead-band region is now approximately doubled while the fuel consumption remains unchanged. A dual-axis system then has a built-in safety factor, in that failure of one or more of the component jets only increases time to damp but does not otherwise affect the damping response.

It is of interest to see how the station inertia ratio influences the rate controlled damping with the pulse-jet stability system. Correspondingly, figure 10 shows  $\tau_{db}$  and  $\epsilon_f$  as functions of  $\gamma$  for the product-of-inertia disturbance and  $\lambda_d = 0.001$ . From the figure both the time to damp and the fuel consumption increase rapidly as the inertia ratio goes from 0.5 (disk distribution) to 1.0 (spherical distribution). An additional increase in the inertia ratio to values greater than 1 (cylindrical distribution) results in a decrease in  $\tau_{db}$  and  $\epsilon_f$ . Thus the jet damper appears to be more effective for disk-shaped or cylindrical station inertias than for near-spherical station inertias.

#### ATTITUDE CONTROL

The pulse-jet system can also be used for attitude control, where both precession and damping torques are necessary. The system control logic then utilizes attitude and rate-error deadbands in producing a station response similar to that shown in figure 11. For this figure, the stability system was actuated with the station at a  $5^\circ$  attitude error. The system then rapidly precessed the station to within the preselected accuracy of  $0.25^\circ$ .

The effect of the system moment level on the time and fuel required to attain the deadband region was also examined for the same initial attitude error. The resulting data are illustrated in figure 12. Both the time to deadband and the fuel consumption now vary with the control moment level. The time to deadband decreases rapidly as the moment level  $\lambda_d$  is increased from 0.00035 to 0.0005 while the fuel consumption is at a minimum at  $\lambda_d = 0.00054$ . Since the time to deadband does not vary appreciably as the moment level is increased, the moment level can be selected to yield the desired minimum fuel consumption without an appreciable increase in time to reorient.

The symmetrical station configuration or inertia ratio again influences the response with the pulse-jet system, as shown on figure 13. For a constant initial attitude error, an increase in the station inertia ratio leads to a corresponding increase in reorientation time without significantly changing the fuel consumption. The disk-like inertia configuration for the symmetric station thus appears to offer the greatest possibilities for rapid and efficient stabilization and reorientation with the pulse-jet system.

It should be noted that no attempt was made to vary the deadband amplitude in attitude control in order to minimize fuel consumption. An optimum system would probably use a variable deadband incorporated in the sensor configuration, and a considerable reduction in fuel consumption is to be expected from this

modification. Further studies aimed at the development of such a sensor configuration are currently being conducted.

#### ATTITUDE CONTROL AND NUTATION DAMPING

Up to now, the pulse-jet system has been actuated primarily by either a station rate or attitude error. The station motion with both an initial attitude error and a product of inertia or applied torque will next be examined. The response of the station with a combined attitude error and applied moment (figs. 11 and 4) is presented in figure 14. Both attitude errors and sinusoidal rate oscillations again occur for the uncontrolled station. With the activation of the pulse-jet system, the body rates and attitude errors are reduced to their deadbands in approximately 18 spin cycles. The rate and attitude deadbands here were selected as before. The rate error deadband can be chosen arbitrarily and is restricted only by the jet response time, while the attitude error deadband must be greater than the maximum expected body-referenced rotation of the principal axes of inertia to avoid excessive fuel consumption. The damped condition for the station will now correspond to a steady spin about an axis within the attitude error deadband. Figure 15 shows the motion of the station resulting from an attitude error and a static product-of-inertia disturbance (figs. 11 and 5). The station wobble and attitude errors are again brought within the respective deadbands. Rate damping is achieved in approximately 7 spin cycles and the final attitude is reached in about 70 spin cycles.

The time history of the station motion for an initial attitude error and a transient product-of-inertia disturbance (figs. 10 and 5) is illustrated in figure 16. The station here damps to its rate error deadband in 3 spin cycles and reaches its final attitude in 43 spin cycles. The pulse-jet system thus is capable of reducing the rate and attitude errors to the selected deadbands for all the disturbances considered.

#### CONCLUDING REMARKS

The results of a computer study on a pulse-jet stability system for a rotating manned space vehicle indicate that the on-off system is capable of damping the wobbling motions of the vehicle and of reorienting the vehicle to within specified limits. The system can be used for nutation damping, attitude control, and combined damping and attitude control. Failure of one or more of the component jets only increases the time to reach the selected attitude and rate limits, but does not otherwise affect the system response. Depending on the duration of the space vehicle mission, the proposed system can be used either for complete stabilization of the vehicle or for attitude control in conjunction with a rate-damping device.

Langley Research Center,  
National Aeronautics and Space Administration,  
Langley Station, Hampton, Va., December 15, 1964.

# APPENDIX

## EQUATIONS OF MOTION

The rigid-body equations for a rotating spacecraft may be written by using a nondimensional time  $\tau$ , an inertia matrix  $\gamma$ , and a moment vector  $\lambda$  denoted by

$$\tau = \Omega_{Z,0} t \quad \tilde{\gamma} = \frac{\tilde{I}}{I_{Z,0}} \quad \bar{\lambda} = \bar{\lambda}_a + \bar{\lambda}_d = \frac{\bar{M}_a + \bar{M}_d}{I_{Z,0} \Omega_{Z,0}^2} \quad (A1)$$

The nondimensional angular-velocity vector then is

$$\bar{\omega} = \frac{d\alpha}{d\tau} = \frac{d\alpha}{dt} \frac{dt}{d\tau} = \frac{\bar{\Omega}}{\Omega_{Z,0}} \quad (A2)$$

and similarly

$$\left. \begin{aligned} \dot{\bar{\omega}} &= \frac{d\bar{\omega}}{d\tau} = \frac{\dot{\bar{\Omega}}}{\Omega_{Z,0}^2} \\ \dot{\bar{\lambda}} &= \frac{d\bar{\lambda}}{d\tau} = \frac{\dot{\tilde{I}}}{I_{Z,0} \Omega_{Z,0}^2} \end{aligned} \right\} \quad (A3)$$

The scalar equations of motion with these nondimensional parameters become

$$\left. \begin{aligned} \lambda_X &= \gamma_X \dot{\omega}_X - \gamma_{XY} \dot{\omega}_Y - \gamma_{XZ} \dot{\omega}_Z + \dot{\gamma}_X \omega_X - \dot{\gamma}_{XY} \omega_Y - \dot{\gamma}_{XZ} \omega_Z - \omega_Z (\gamma_Y \omega_Y - \gamma_{YZ} \omega_Z - \gamma_{YX} \omega_X) + \omega_Y (\gamma_Z \omega_Z - \gamma_{ZX} \omega_X - \gamma_{ZY} \omega_Y) \\ \lambda_Y &= \gamma_Y \dot{\omega}_Y - \gamma_{YZ} \dot{\omega}_Z - \gamma_{YX} \dot{\omega}_X + \dot{\gamma}_Y \omega_Y - \dot{\gamma}_{YZ} \omega_Z - \dot{\gamma}_{YX} \omega_X - \omega_X (\gamma_Z \omega_Z - \gamma_{ZX} \omega_X - \gamma_{ZY} \omega_Y) + \omega_Z (\gamma_X \omega_X - \gamma_{XY} \omega_Y - \gamma_{XZ} \omega_Z) \\ \lambda_Z &= \gamma_Z \dot{\omega}_Z - \gamma_{ZX} \dot{\omega}_X - \gamma_{ZY} \dot{\omega}_Y + \dot{\gamma}_Z \omega_Z - \dot{\gamma}_{ZX} \omega_X - \dot{\gamma}_{ZY} \omega_Y - \omega_Y (\gamma_X \omega_X - \gamma_{XY} \omega_Y - \gamma_{XZ} \omega_Z) + \omega_X (\gamma_Y \omega_Y - \gamma_{YZ} \omega_Z - \gamma_{YX} \omega_X) \end{aligned} \right\} \quad (A4)$$

and the inertias in these equations can be defined in terms of arbitrary moving masses within the spacecraft (ref. 4).

The nondimensional angular velocities obtained from equation (A4) give the Euler angle rates

# APPENDIX

$$\left. \begin{aligned} \frac{d\phi}{d\tau} &= \omega_X + \omega_Y \tan \theta \sin \phi + \omega_Z \tan \theta \cos \phi \\ \frac{d\theta}{d\tau} &= \omega_Y \cos \phi - \omega_Z \sin \phi \\ \frac{d\psi}{d\tau} &= \omega_Z \cos \phi \sec \theta + \omega_Y \sin \phi \sec \theta \end{aligned} \right\} \quad (A5)$$

where

$$\frac{d\phi}{d\tau} = \frac{\dot{\phi}}{\Omega_{Z,0}} \quad \frac{d\theta}{d\tau} = \frac{\dot{\theta}}{\Omega_{Z,0}} \quad \frac{d\psi}{d\tau} = \frac{\dot{\psi}}{\Omega_{Z,0}} \quad (A6)$$

Numerical integration of equations (A4) and (A5) then yields the motion of the spacecraft for specified applied torques and product-of-inertia disturbances.

For this analysis the position of the spacecraft is given in terms of a set of stability angles. These angles are similar to the angles that would be measured by a solar sensor system in the actual spacecraft.

The stability angles  $U$ ,  $V$ , and  $W$  are shown in figure 3, and are given by

$$U = \cos^{-1}(\cos \phi \cos \theta)$$

$$V = -\theta$$

$$W = \sin^{-1}(\sin \phi \cos \theta)$$

where  $U$  is defined as the inclination angle between the  $Z$  body axis and  $Z$  fixed-space axis, and  $V$  and  $W$  are the angles the  $X$  body axis and  $Y$  body axis make with the  $XY$  fixed-space reference plane. These angles provide a simple means of determining the deviation of the body axes from a fixed reference plane and position.

## REFERENCES

1. Grantham, William D.: Effects of Mass-Loading Variations and Applied Moments on Motion and Control of a Manned Space Vehicle. NASA TN D-803, 1961.
2. Suddath, Jerrold H.: A Theoretical Study of the Angular Motions of Spinning Bodies in Space. NASA TR R-83, 1961.
3. Martz, William C.: Method for Approximating the Vacuum Motions of Spinning Symmetrical Bodies with Nonconstant Spin Rates. NASA TR R-115, 1961.
4. Kurzahls, Peter R.; and Keckler, Claude R.: Spin Dynamics of Manned Space Stations. NASA TR R-155, 1963.
5. Adams, J. J.: Study of an Active Control System for a Spinning Body. NASA TN D-905, 1961.
6. Haseltine, W. R.: Passive Damping of Wobbling Satellites - Part 1. General Stability Theory and First Example. NAVORD Rept. 6579, Pt. 1 (NOTS TP 2306), U.S. Naval Ord. Test Station (China Lake, Calif.), July 31, 1959.

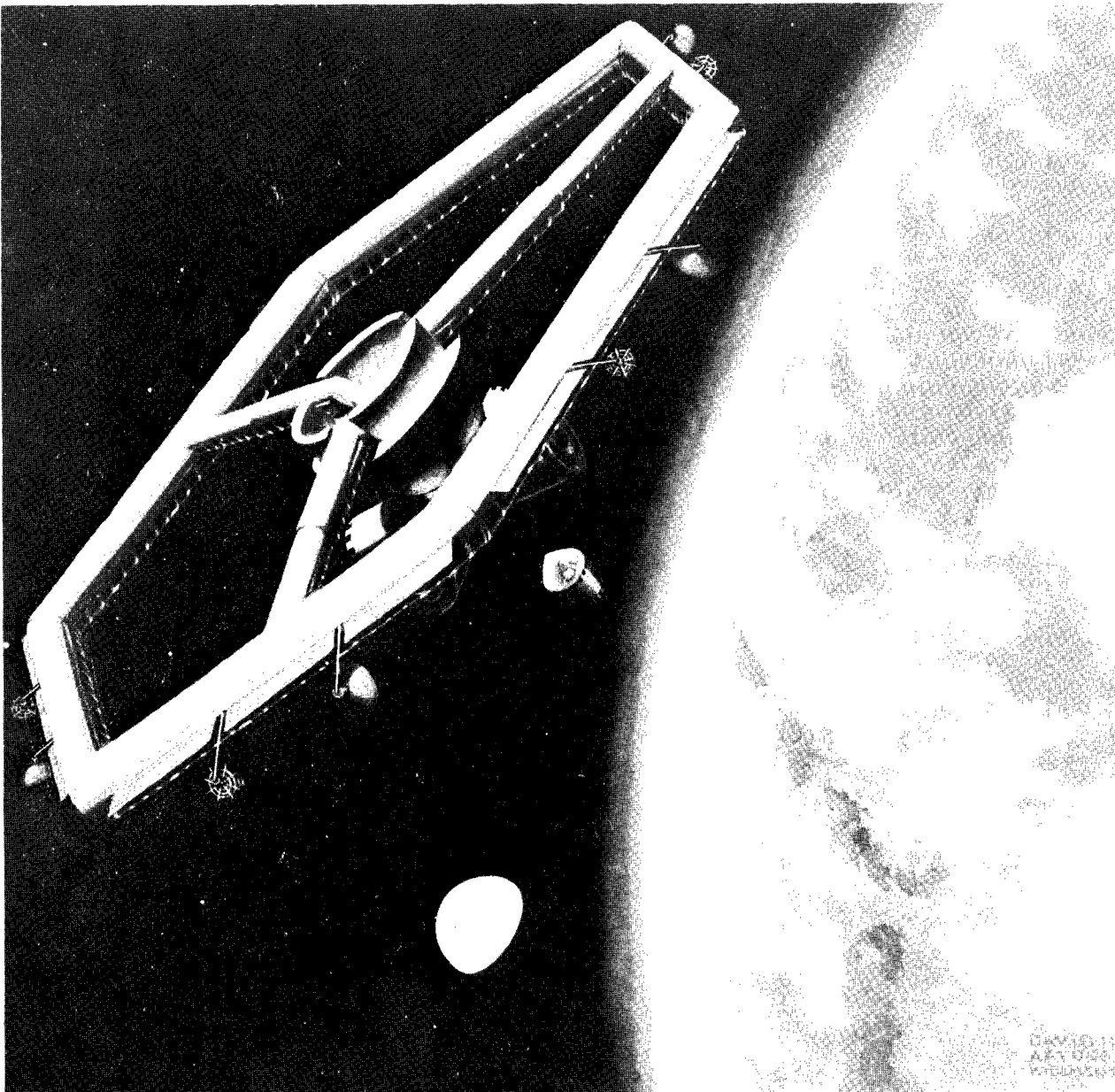


Figure 1.- Painting of possible space station.

L-62-8400

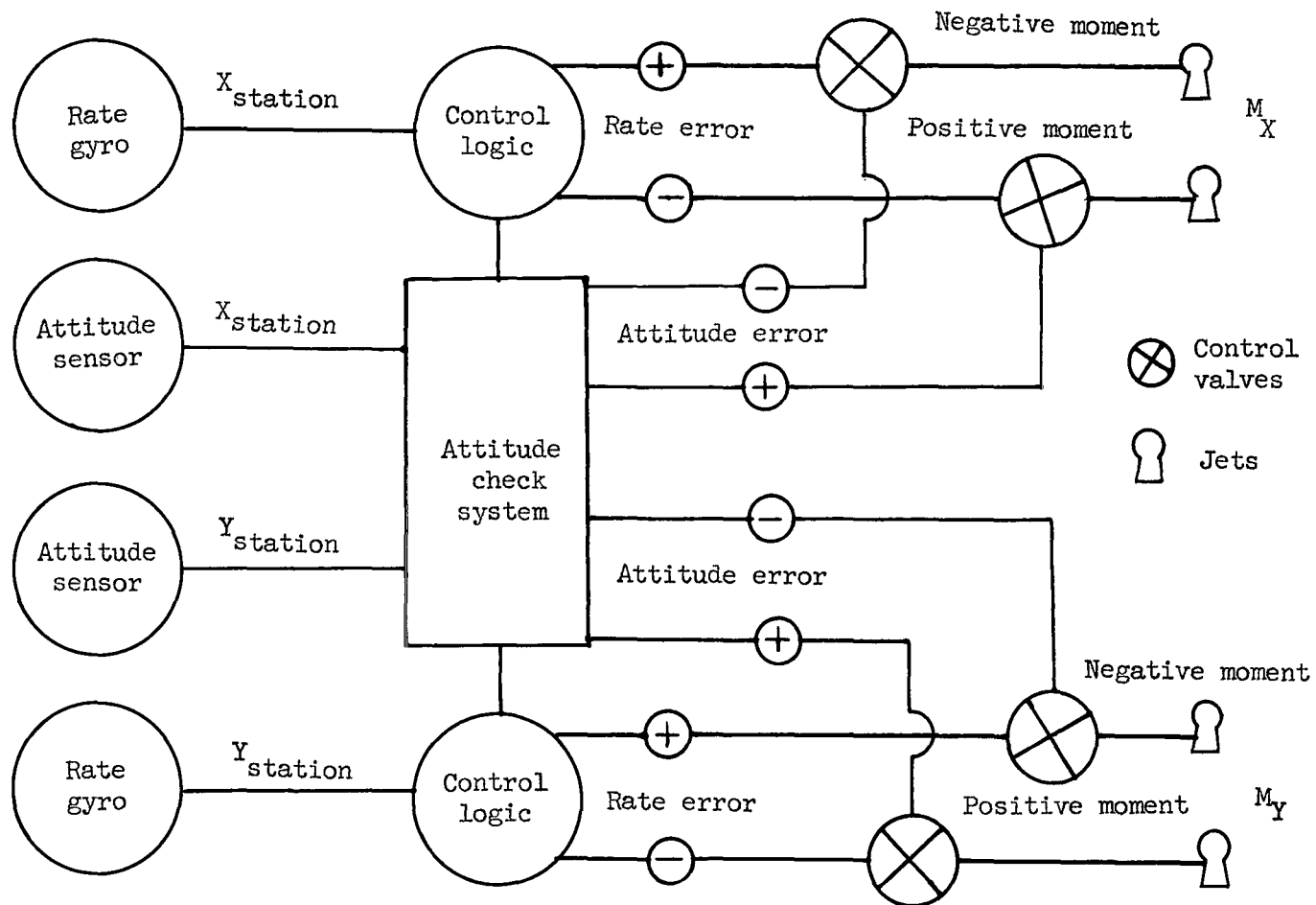


Figure 2.- Block diagram of pulse-jet system.



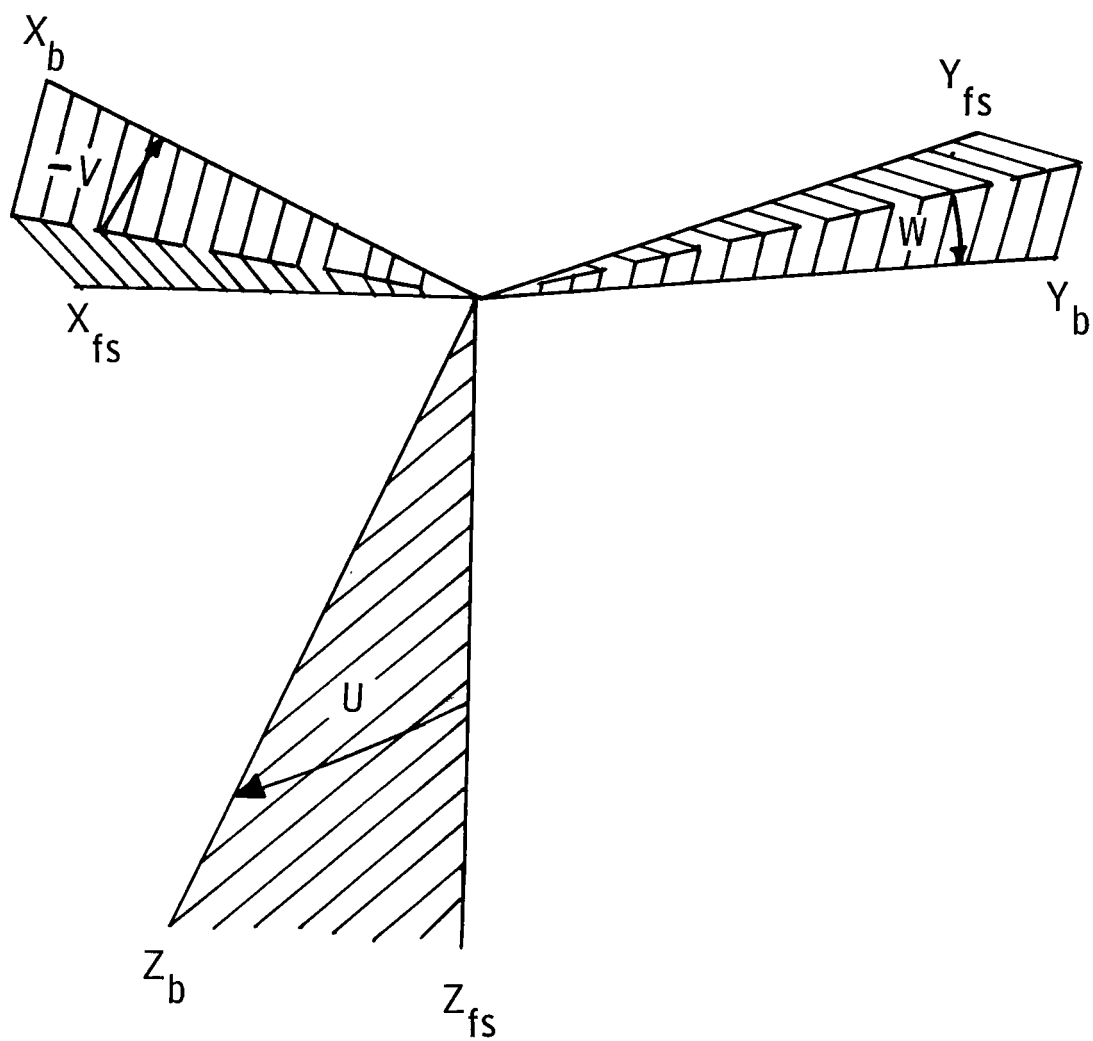


Figure 3.- Orientation of body axes with respect to space-fixed axes by means of stability angles.

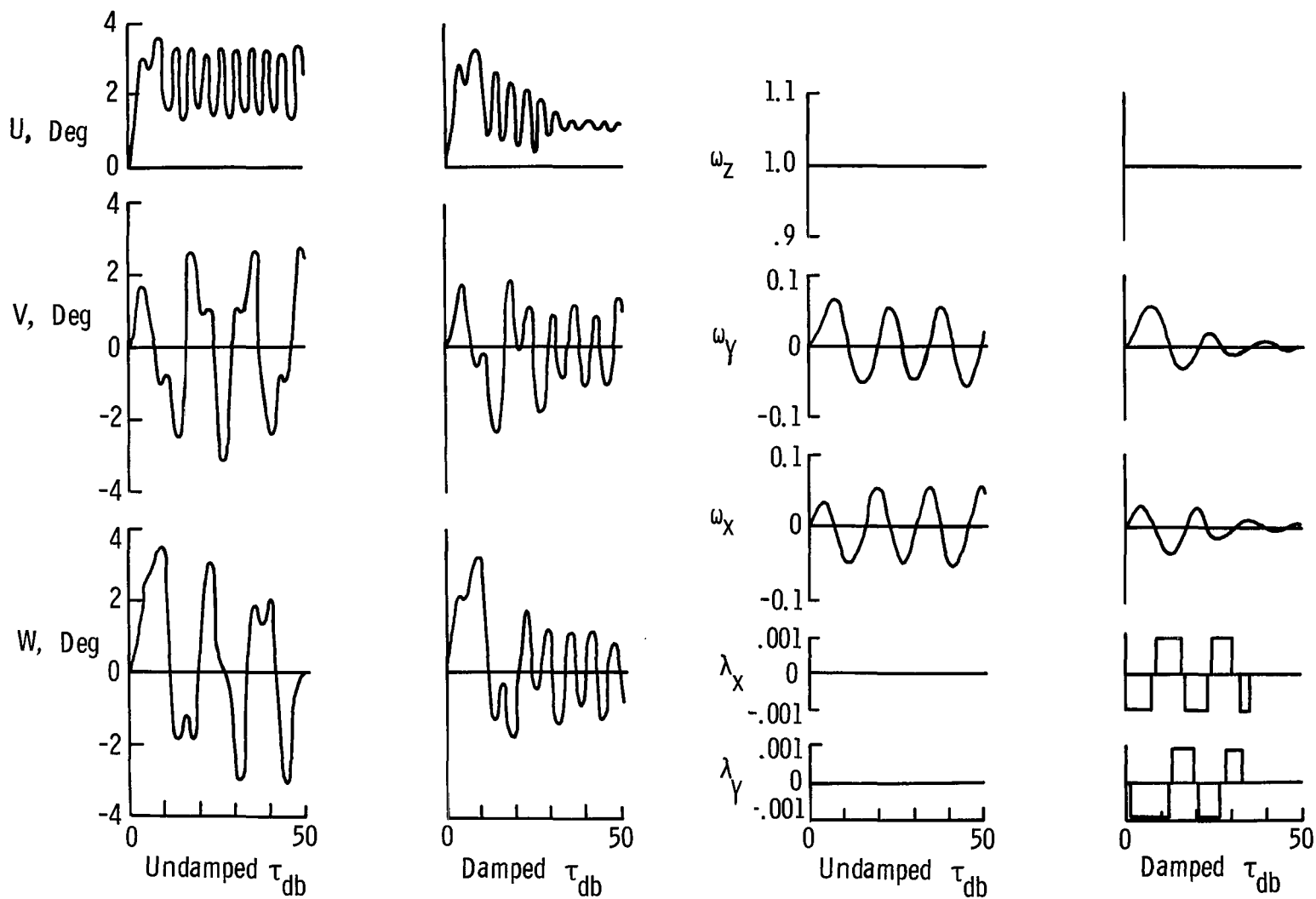


Figure 4.- Motion of station resulting from docking torque with a rate-controlled stability system.

$$\epsilon_F = 0.073; A = 0.0005\Omega_Z; \gamma = 0.70; \lambda_d = 0.001.$$

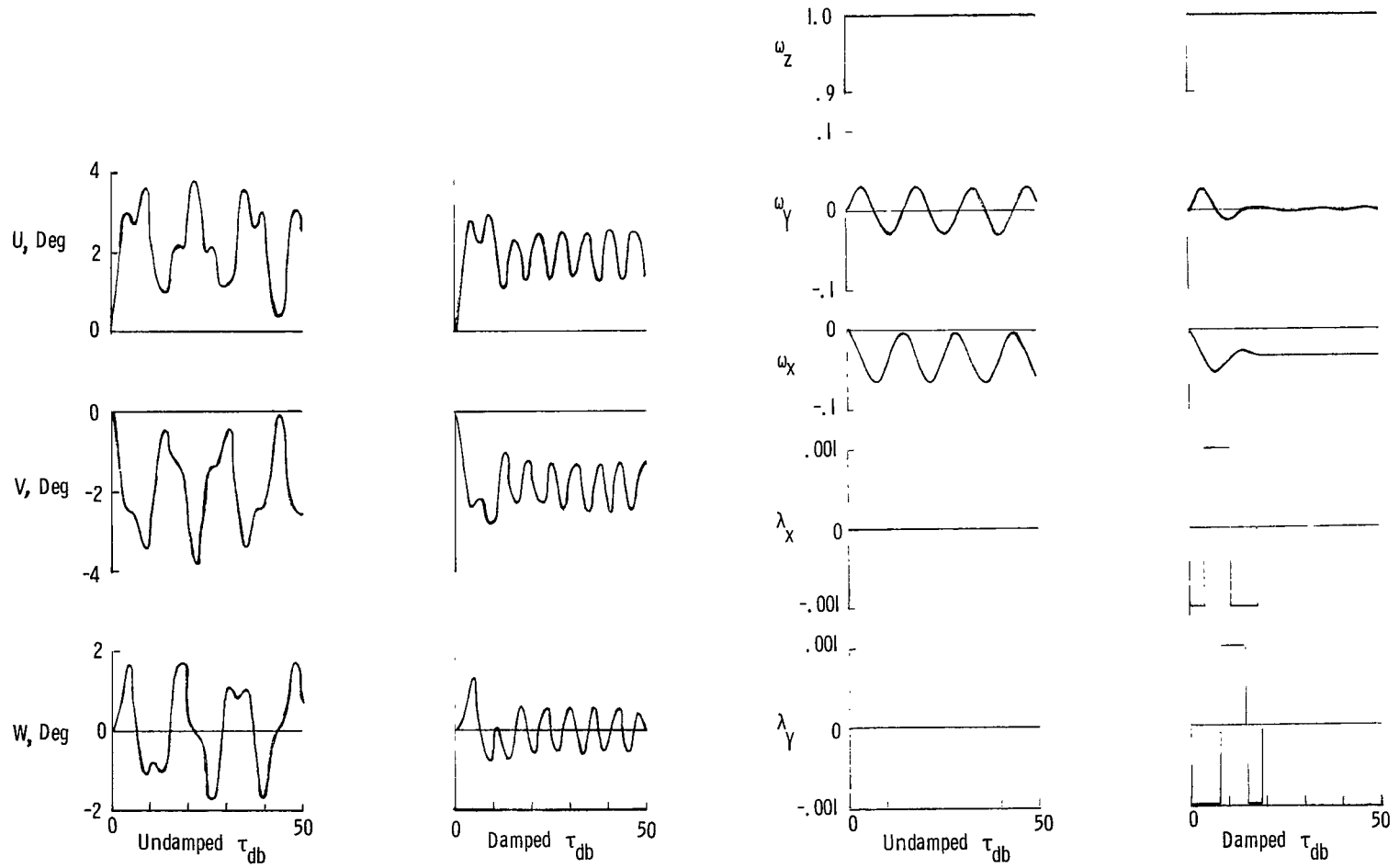


Figure 5.- Motion of station with a product of inertia and the rate-controlled pulse-set system.  
 $A = 0.0005\Omega_z$ ;  $\lambda_d = 0.001$ ;  $\gamma = 0.70$ ;  $I_{xz}/I_z = 0.01$ ;  $\epsilon_F = 0.035$ .

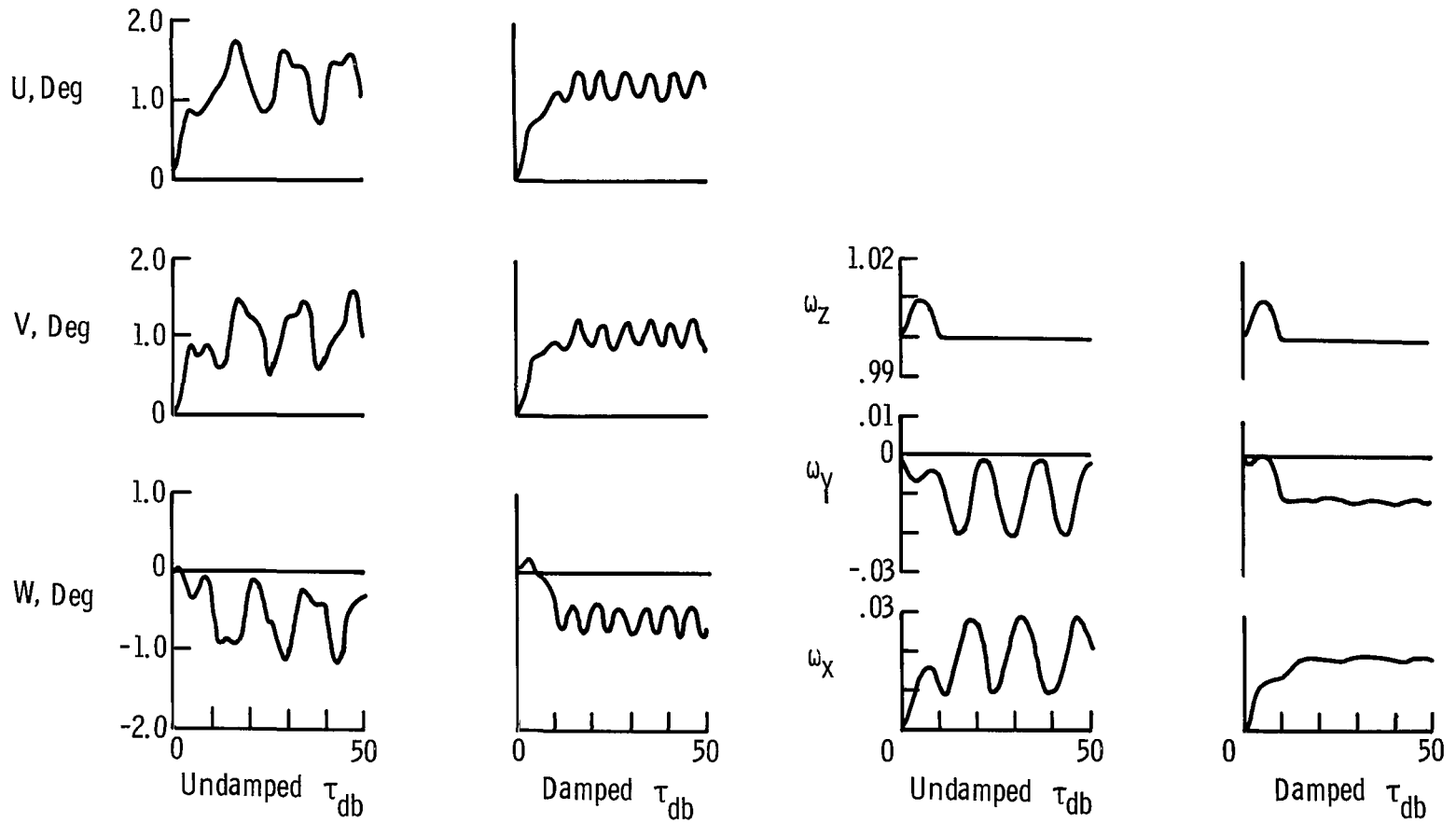


Figure 6.- Motion of station with a transient product of inertia disturbance and rate-controlled stability system.  $A = 0.0005\Omega_z$ ;  $\gamma = 0.70$ ;  $\lambda_d = 0.001$ ;  $\epsilon_F = 0.0256$ .

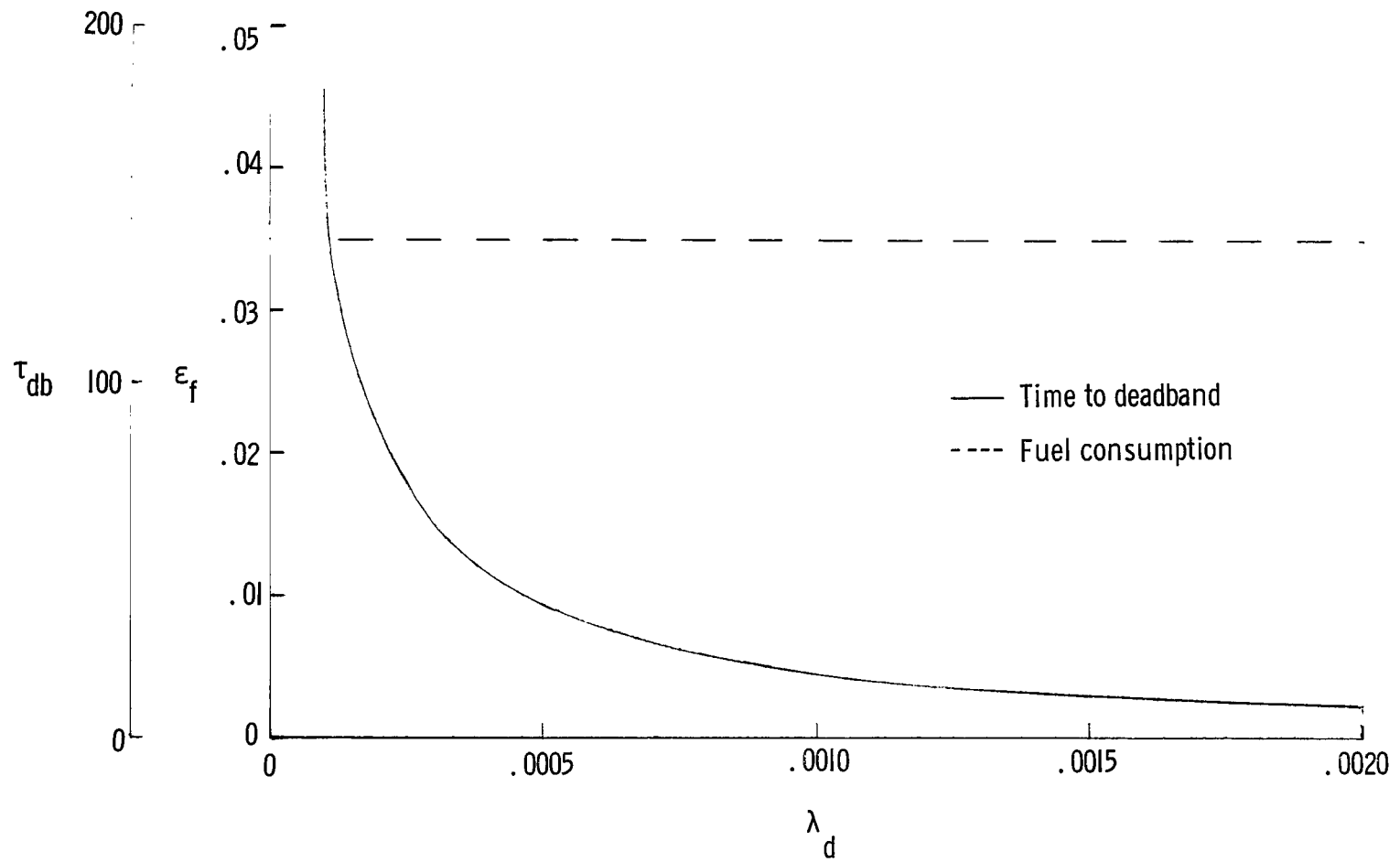


Figure 7.- Variation of system damping parameters with rate-controlled moment level.  
 $A = 0.0005\Omega_z$ ;  $\gamma = 0.7$ ;  $I_{xz}/I_z = 0.01$ .

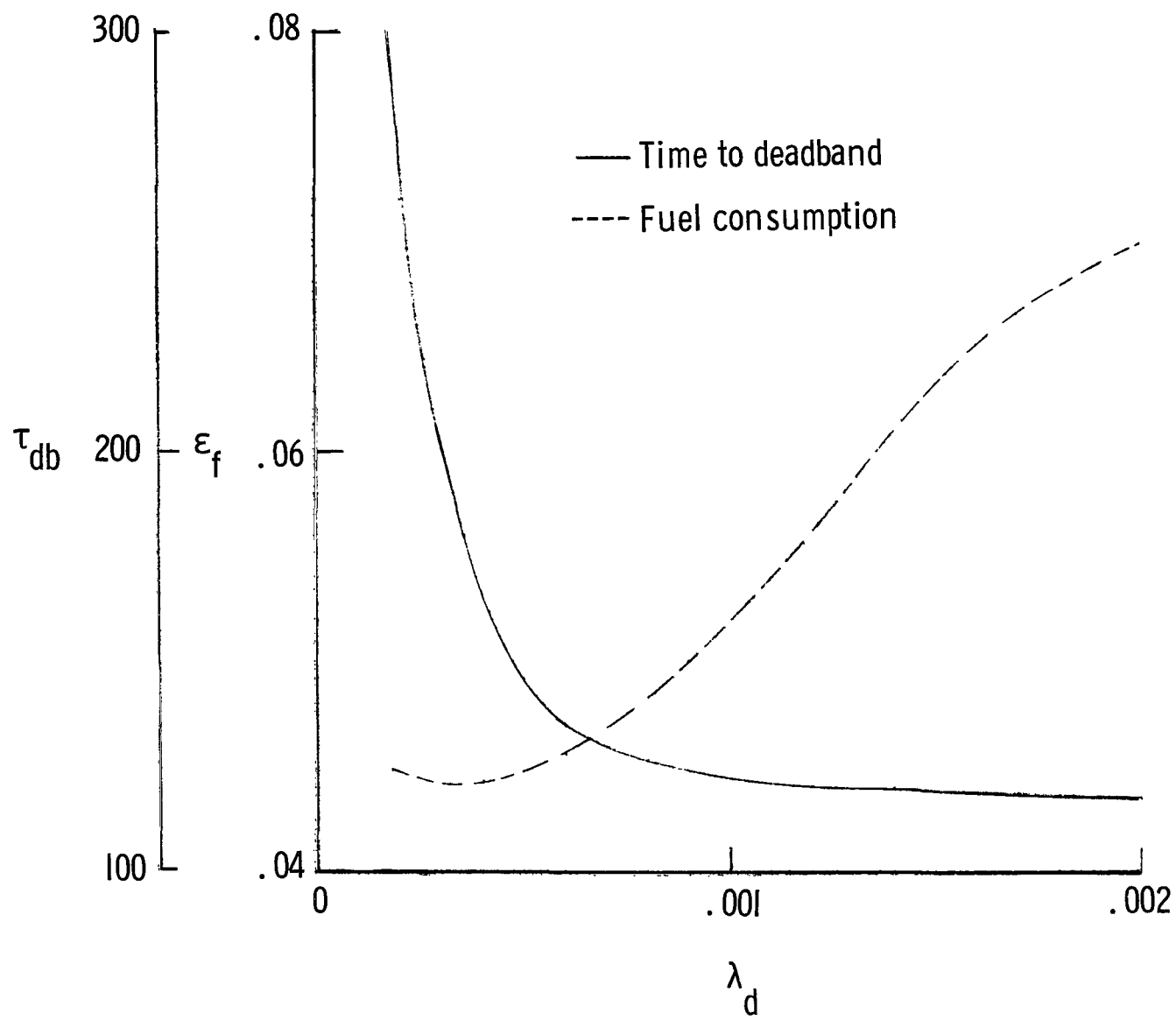


Figure 8.- Variation of pulse-jet damping parameters with control-moment level.  
 $A = 0.0005 \Omega_z$ ;  $\gamma = 0.7$ ;  $I_{xz}/I_z = 0.01$ ;  $B = 1.95$  deg.

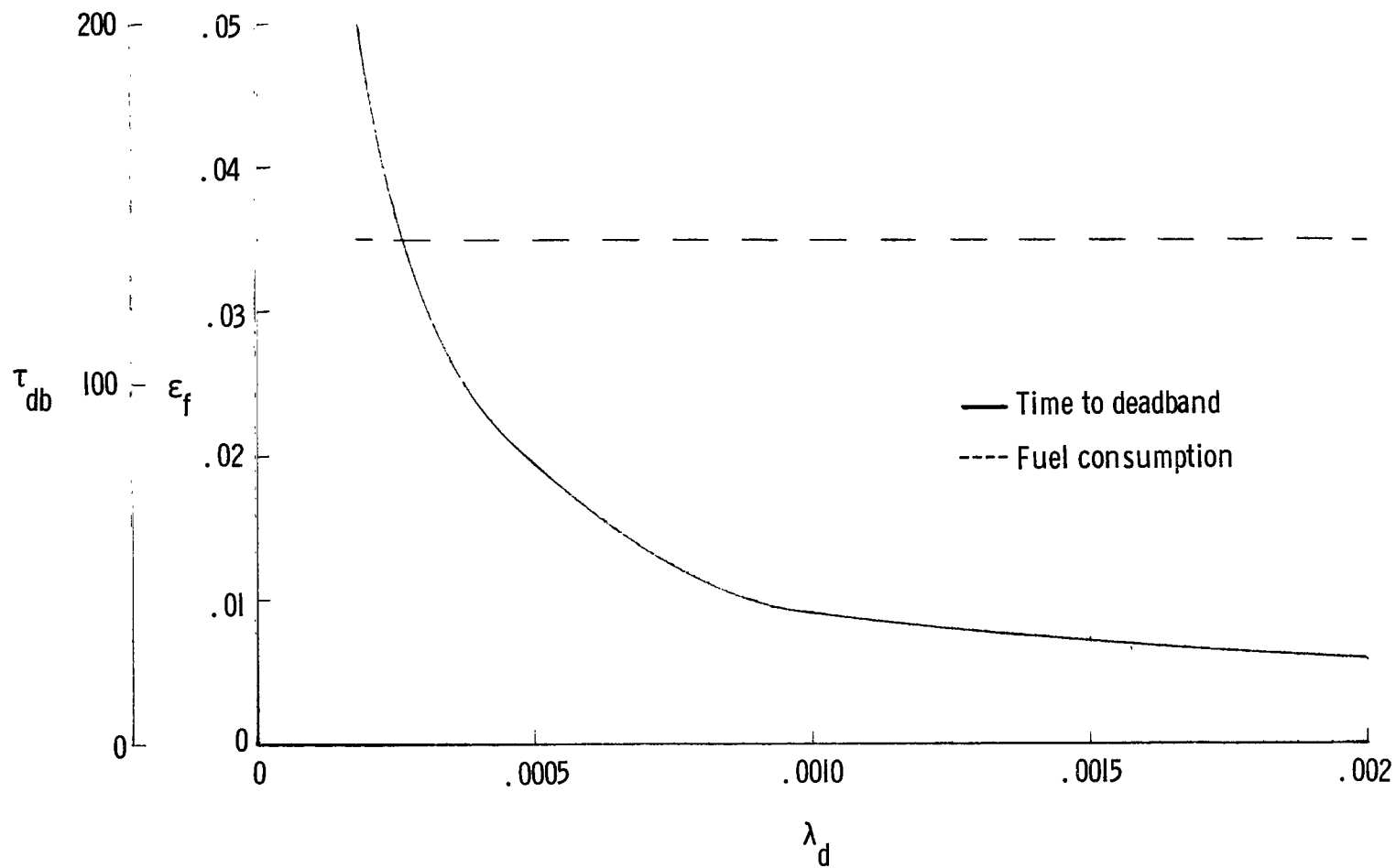


Figure 9.- Variation of pulse-jet damping parameters with single-axis control-moment level.  $A = 0.0005\Omega_z$ ;  $\gamma = 0.7$ ;  $I_{xz}/I_z = 0.01$ .

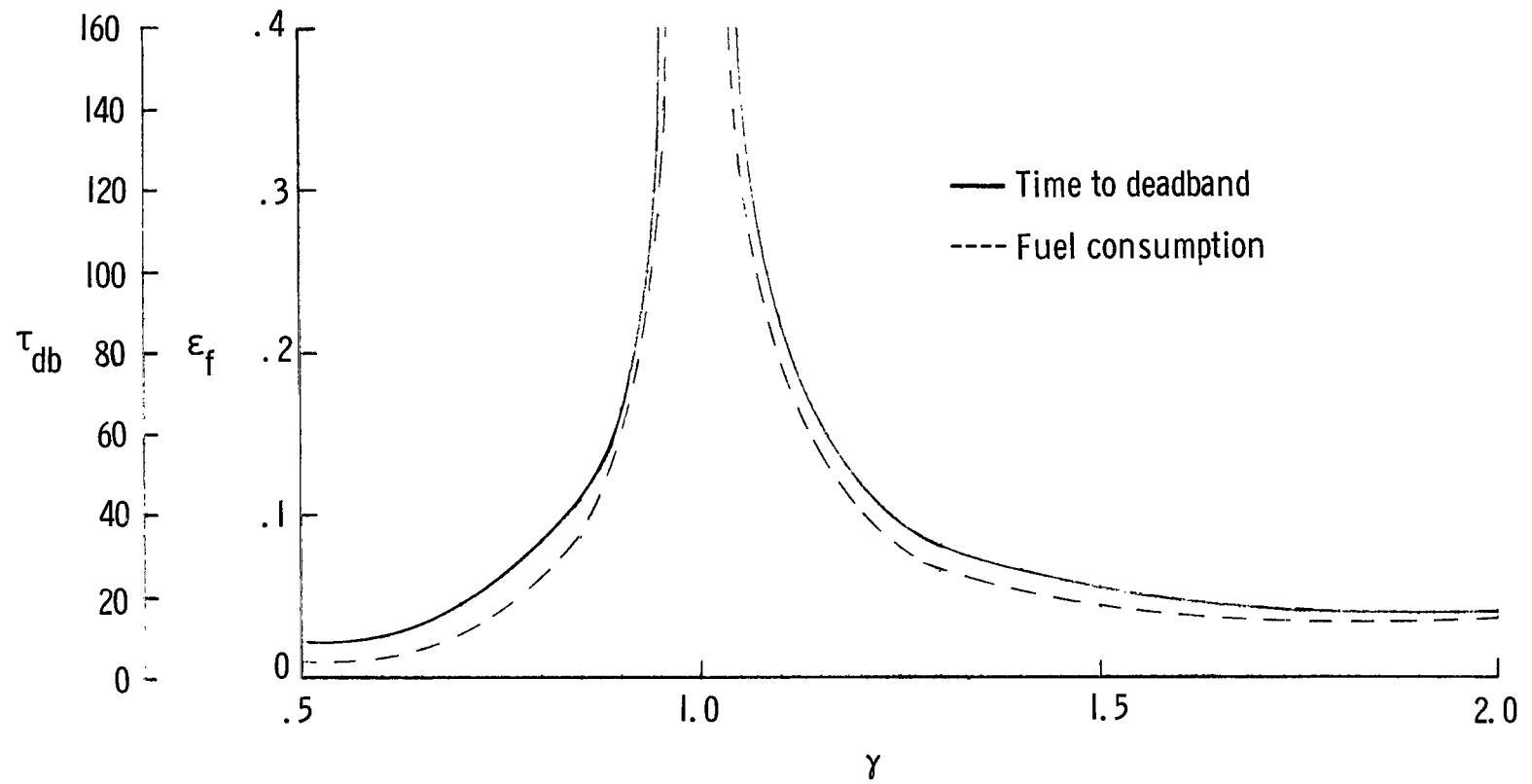


Figure 10.- Variation of pulse-jet damping parameters with station inertia ratio.  
 $A = 0.0005\Omega_Z$ ;  $\lambda_d = 0.001$ ;  $I_{XZ}/I_Z = 0.01$ .



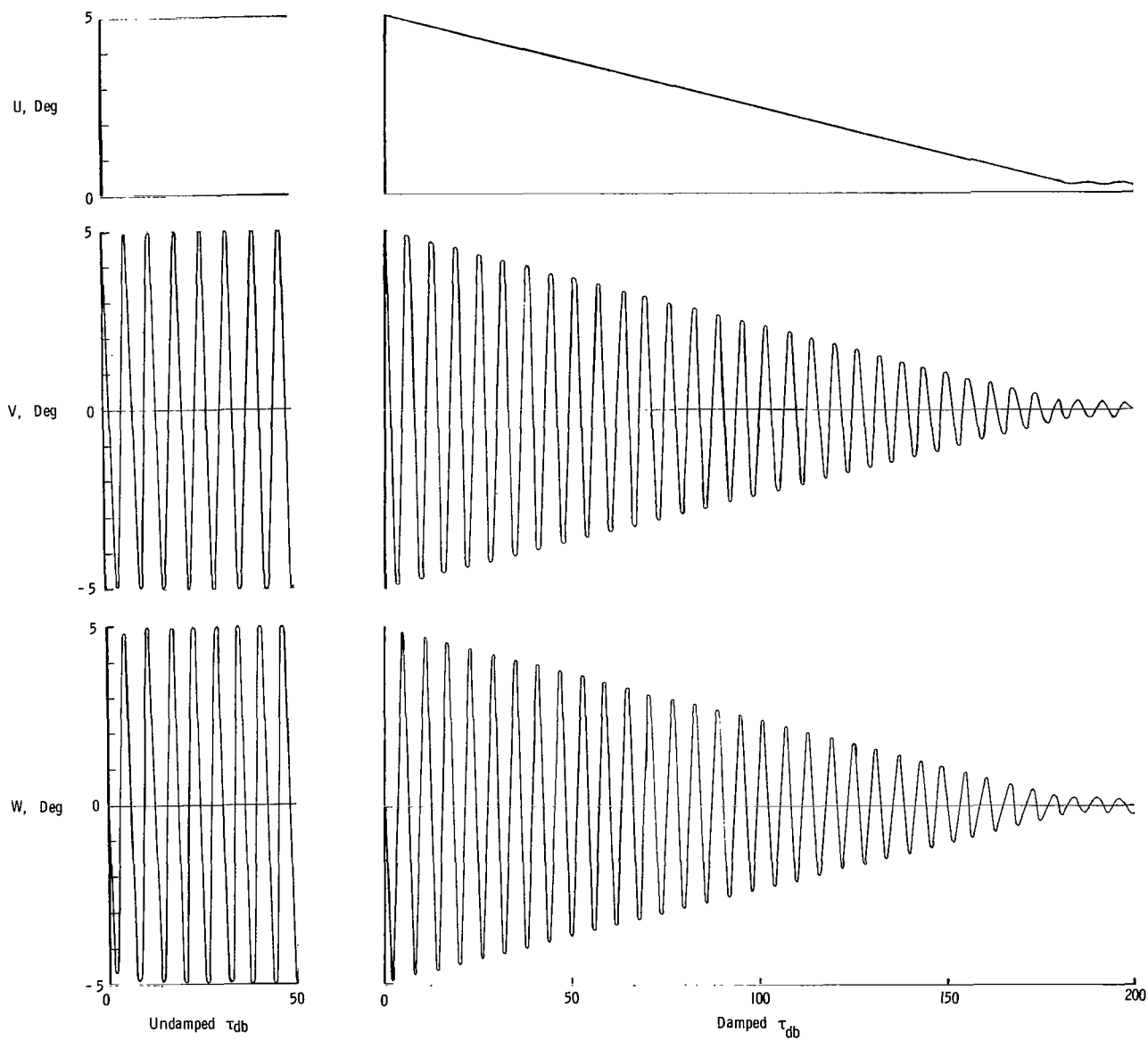


Figure 11.- Motion of station with an initial attitude error and the rate-attitude controlled pulse-jet system.  $A = 0.0005 \Omega_z$ ;  $B = 0.25$  deg;  $\gamma = 0.7$ ;  $\lambda_d = 0.001$ ;  $U = 5$  deg;  $\epsilon_F = 0.132$ .

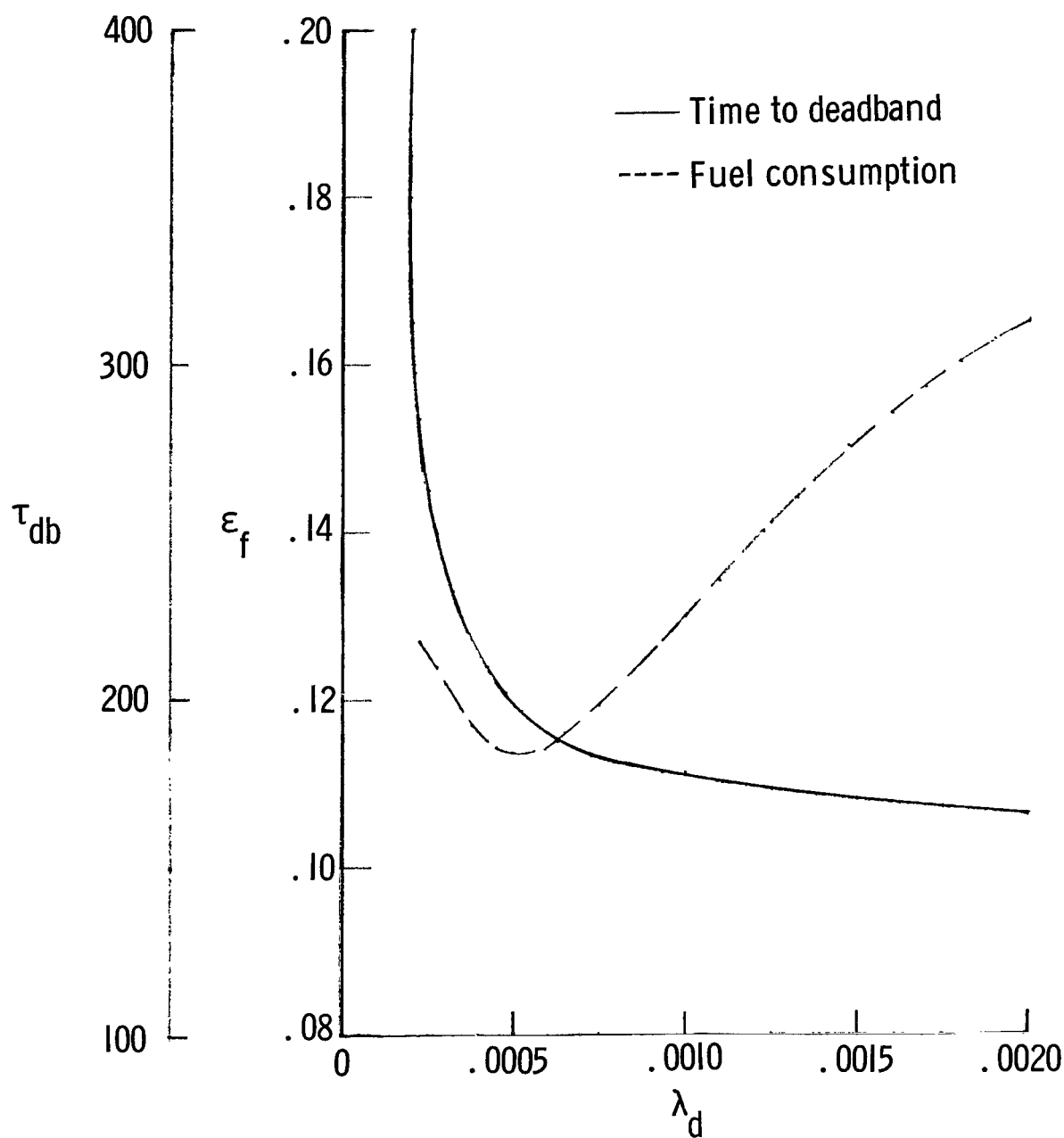


Figure 12.- Variation of pulse-jet orientation parameters with control-moment level.  
 $A = 0.0005 \Omega_z$ ;  $B = 0.25$  deg;  $\gamma = 0.7$ ;  $U = 5$  deg.

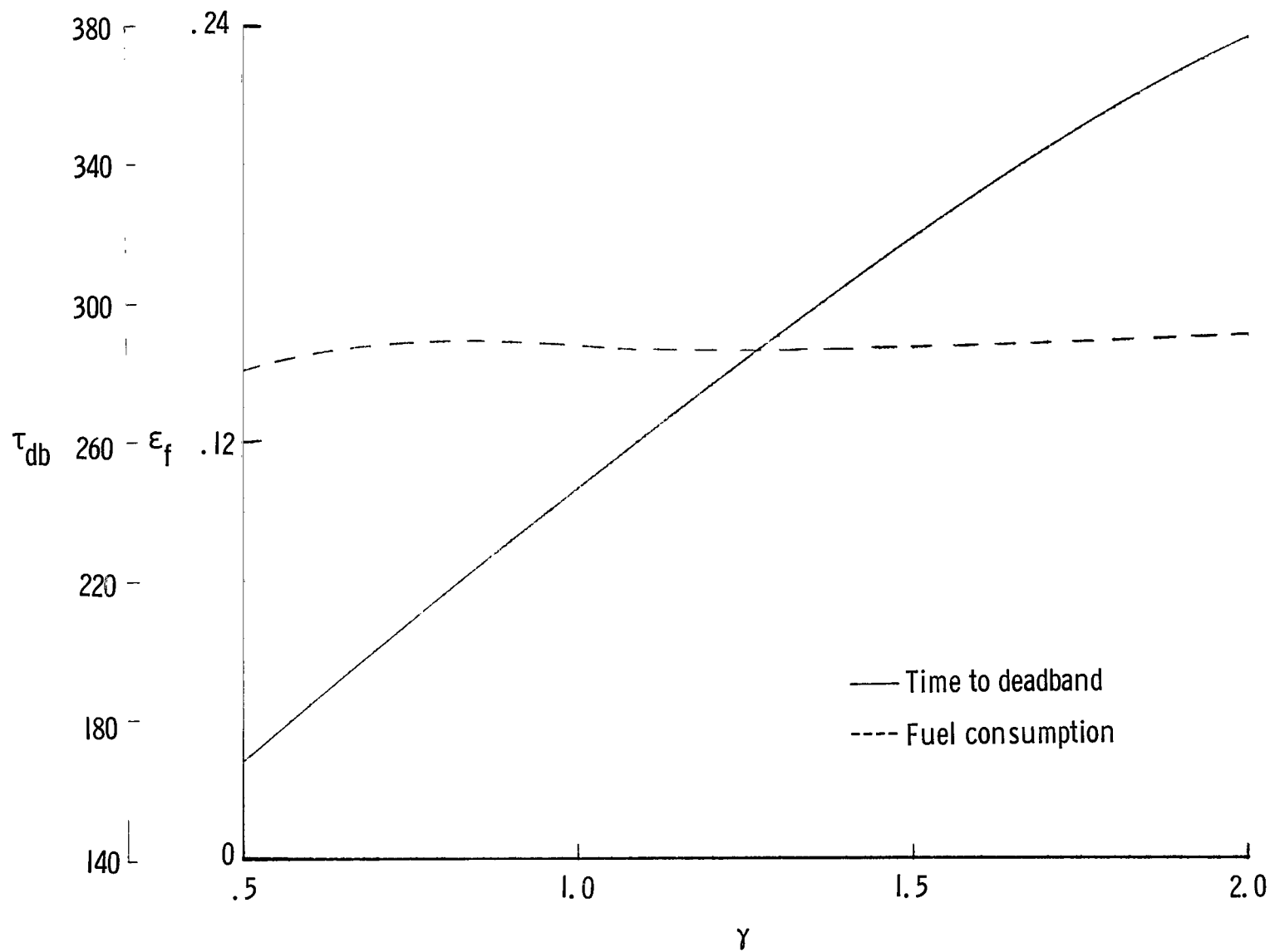


Figure 13.- Variation of pulse-jet orientation parameters with station inertia ratio.  
 $A = 0.0005\Omega_z$ ;  $\lambda_d = 0.001$ ;  $B = 0.25$  deg;  $U = 5$  deg.

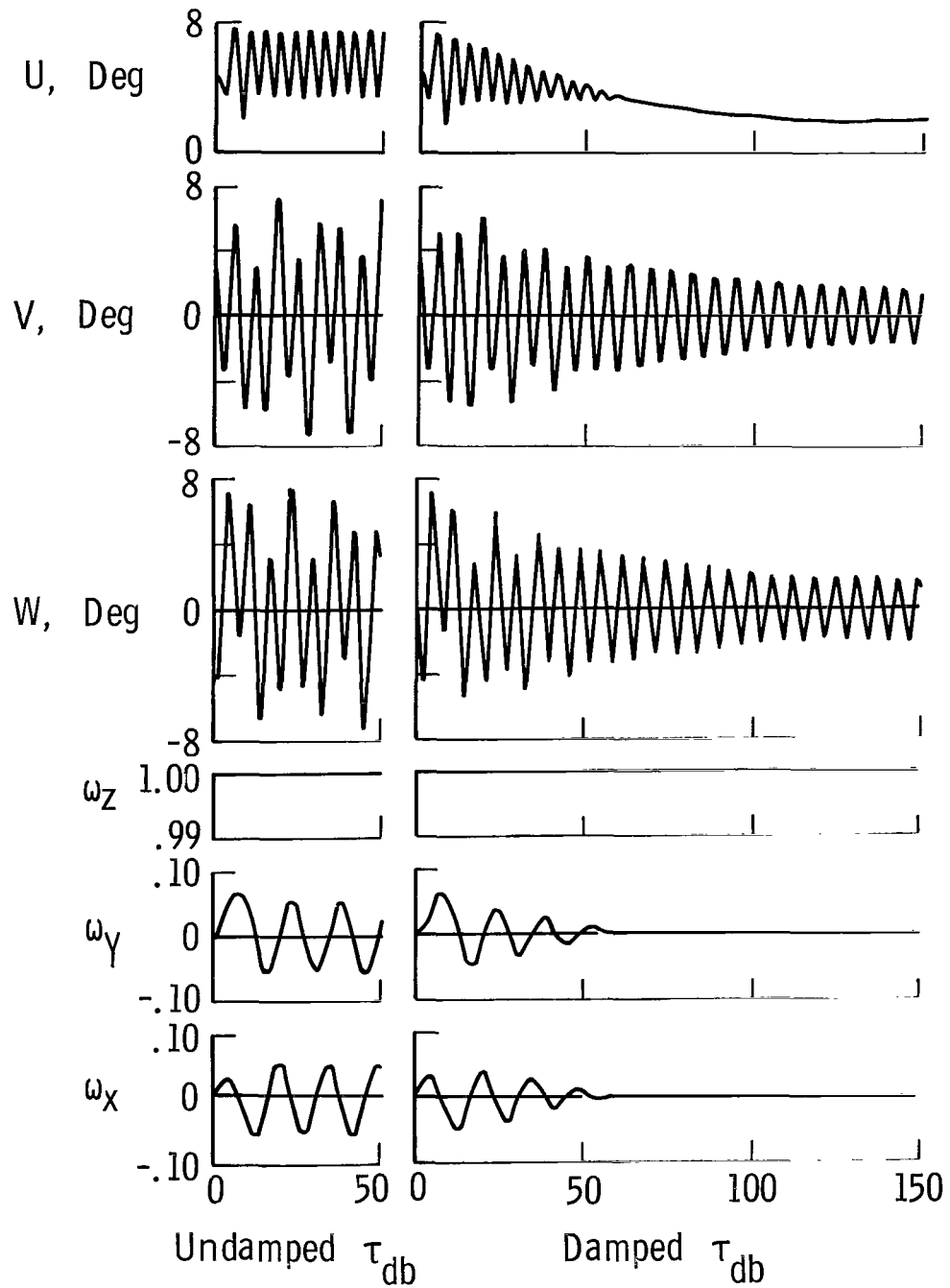


Figure 14.- Motion of station with an initial attitude error and an applied moment.  
 $A = 0.0005\Omega_z$ ;  $\gamma = 0.7$ ;  $\lambda_d = 0.001$ ;  $U = 5$  deg;  $\epsilon_f = 0.1207$ ;  $B = 1.95$  deg.

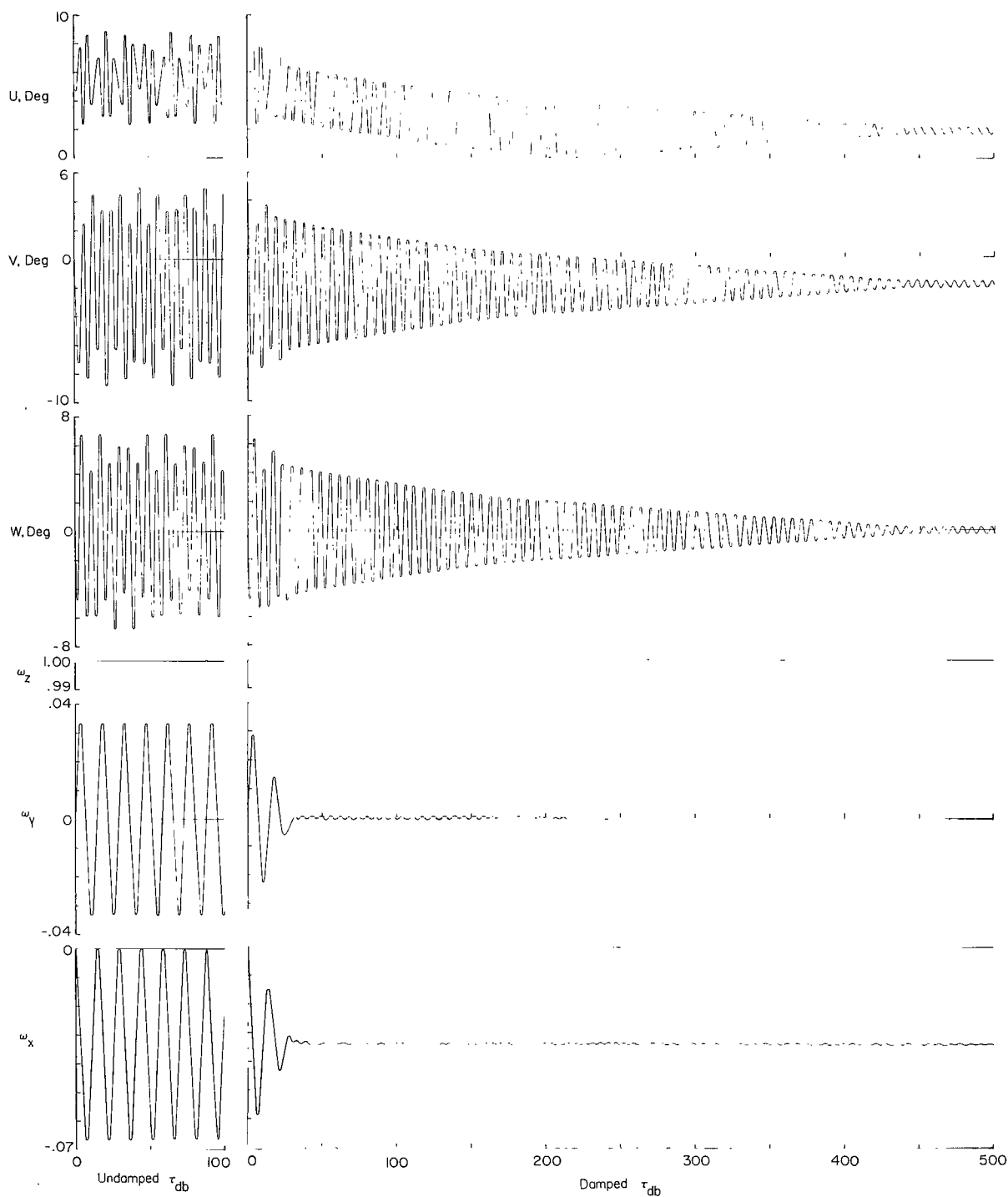


Figure 15.- Motion of station with an initial attitude error and a static product of inertia.  $\epsilon_F = 0.183$ ;  $A = 0.0005 \Omega_Z$ ;  $U = 5$  deg;  $I_{XZ}/I_Z = 0.01$ ;  $B = 2.05$  deg;  $\lambda_d = 0.001$ ;  $\gamma = 0.7$ .

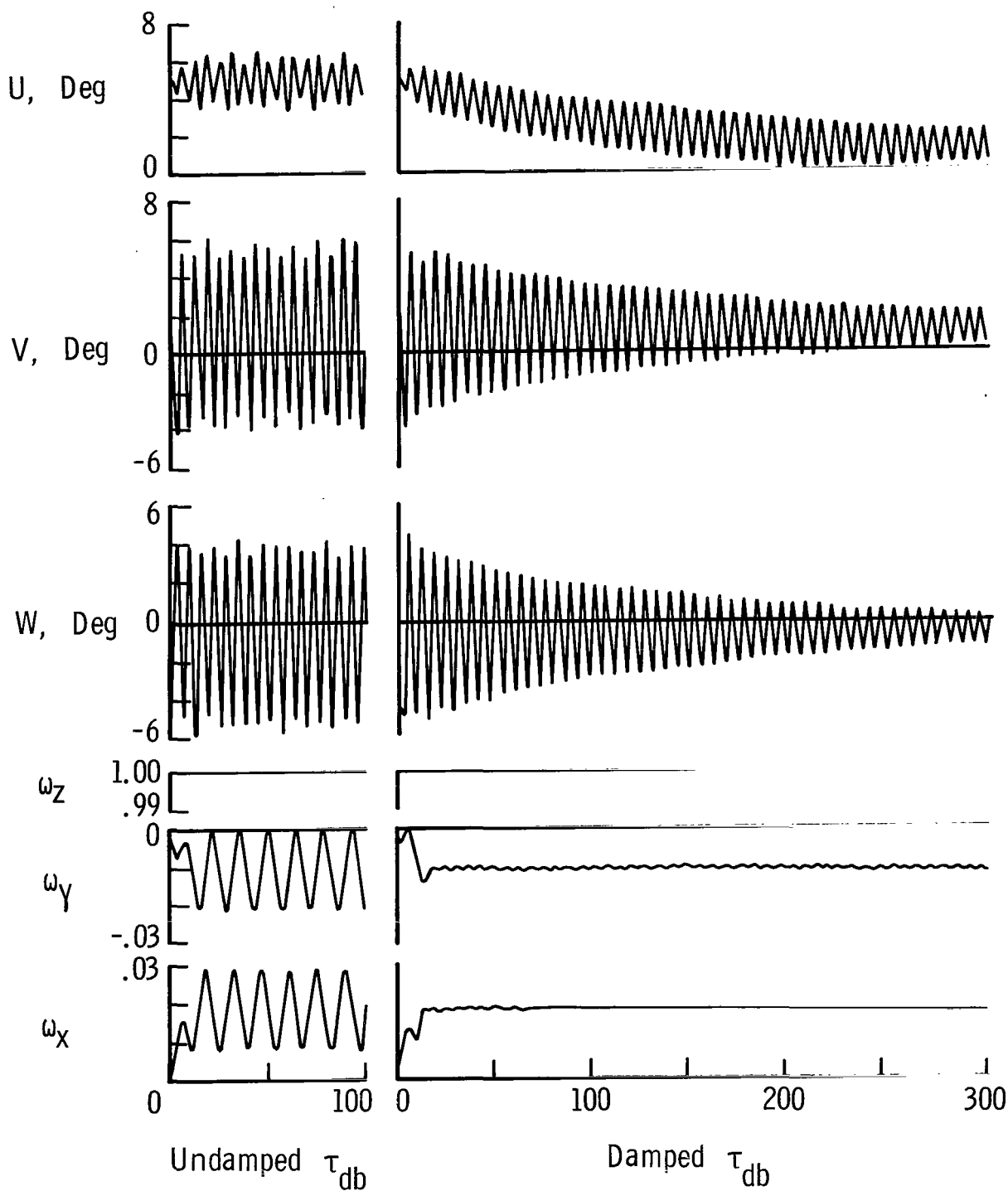


Figure 16.- Motion of station with an initial attitude error and a transient product-of-inertia disturbance.  $A = 0.0005\Omega_z$ ;  $U = 5$  deg;  $\lambda_d = 0.001$ ;  $B = 1.95$  deg;  $\epsilon_F = 0.116$ ;  $\gamma = 0.7$ .

2/22/85  
8

*"The aeronautical and space activities of the United States shall be conducted so as to contribute . . . to the expansion of human knowledge of phenomena in the atmosphere and space. The Administration shall provide for the widest practicable and appropriate dissemination of information concerning its activities and the results thereof."*

—NATIONAL AERONAUTICS AND SPACE ACT OF 1958

## NASA SCIENTIFIC AND TECHNICAL PUBLICATIONS

**TECHNICAL REPORTS:** Scientific and technical information considered important, complete, and a lasting contribution to existing knowledge.

**TECHNICAL NOTES:** Information less broad in scope but nevertheless of importance as a contribution to existing knowledge.

**TECHNICAL MEMORANDUMS:** Information receiving limited distribution because of preliminary data, security classification, or other reasons.

**CONTRACTOR REPORTS:** Technical information generated in connection with a NASA contract or grant and released under NASA auspices.

**TECHNICAL TRANSLATIONS:** Information published in a foreign language considered to merit NASA distribution in English.

**TECHNICAL REPRINTS:** Information derived from NASA activities and initially published in the form of journal articles.

**SPECIAL PUBLICATIONS:** Information derived from or of value to NASA activities but not necessarily reporting the results of individual NASA-programmed scientific efforts. Publications include conference proceedings, monographs, data compilations, handbooks, sourcebooks, and special bibliographies.

*Details on the availability of these publications may be obtained from:*

SCIENTIFIC AND TECHNICAL INFORMATION DIVISION  
NATIONAL AERONAUTICS AND SPACE ADMINISTRATION  
Washington, D.C. 20546